European Journal of Mechanics A/Solids 63 (2017) 36–42

Contents lists available at ScienceDirect

European Journal of Mechanics A/Solids

journal homepage: www.elsevier.com/locate/ejmsol

Loss of ellipticity in elasticity with energy limiters

K.Y. Volokh

Faculty of Civil and Environmental Engineering, Technion – I.I.T., Israel

ARTICLE INFO

Article history:
Received 12 July 2016
Received in revised form
8 October 2016
Accepted 10 October 2016
Available online 15 October 2016

ABSTRACT

Traditional hyperelastic models usually obey requirement of material stability in various forms: Baker-Ericksen inequalities, strong ellipticity, polyconvexity etc. It is reasonable, of course, to require stability for the intact behavior of materials. However, all materials fail and a description of failure should be incorporated in the constitutive law. A simple version of hyperelasticity with failure can be formulated based on the introduction of the limiter in the strain energy density. The limited strain energy bounds maximum achievable stress automatically. Evidently, the elasticity with the energy limiter should exhibit material instability.

This work addresses two practically interesting calculations concerning the onset of material instability via the loss of ellipticity. First, we consider simple shear of natural rubber. We find the direction of failure localization, which is in perfect *qualitative* correspondence with fracture observations in rubber bearings after earthquakes. Interestingly, the direction of failure localization is different from the one predicted by the criterion of maximum tension stress or stretch. Second, we consider equibiaxial tension of a sheet of aneurysm material. We find that the isotropic aneurysm material exhibits infinitely many possible directions of failure localization in equibiaxial tension. The latter means that the random direction of cracks in equibiaxial tension experiment, e.g. membrane inflation, can be an indicator of material isotropy. Accordingly, a preferable direction of the crack alignment can be interpreted as an indicator of the aneurysm anisotropy.

1. Introduction

Materials fail. This physical observation was a bit ignored during the development of the theory of elasticity. Indeed, various requirements (Baker-Ericksen inequalities, strong ellipticity, polyconvexity etc.) are often imposed on the constitutive models to prevent from the appearance of material instability and failure. More physical trend emerged recently with regard to a description of fiber-reinforced materials. It was noted that some constitutive models could exhibit material instabilities observed experimentally: Kurashige (1981); Triantafyllidis and Abeyaratne (1983); Danescu (1991); Merodio and Ogden (2002, 2003, 2005); Dorfmann and Ogden (2015).

In parallel, the approach of continuum damage mechanics has been developing, in which a damage variable is introduced to reduce material stiffness: Simo (1987); Simo and Ju (1987); Govindjee and Simo (1991); Johnson and Beatty (1993); Miehe (1995); de Souza Neto et al. (1998); Ogden and Roxburgh (1999); Kaliske et al. (2001); Menzel and Steinmann (2001); Dorfmann and Ogden (2004); Guo and Sluys (2006); De Tommasi et al. (2008); Dal and Kaliske (2009). The damage variable requires definition of an evolution law and damage threshold conditions. The damage variable is the internal one, which means that its interpretation in simple physical terms is not readily available. Nevertheless, the introduction of the damage variable is instrumental when partial material damage gradually develops (like in the case of Mullins effect).

In the cases of the abrupt rupture, much simpler approach free of internal variables can be used based on the introduction of energy limiters (Volokh, 2004, 2007, 2013, 2014). In the latter case, the strain energy is bounded by an energy limiter that enforces saturation – the failure energy. The latter indicates the maximum amount of energy that can be stored and dissipated by an infinitesimal material volume. The limiter induces stress bounds in the constitutive equations automatically. Remarkably, the analysis of the onset of material instability becomes simple in the absence of internal variables.

Evidently, the strong ellipticity restriction should be violated for the material model incorporating a failure description. However,

E-mail address: cvolokh@technion.ac.il.

http://dx.doi.org/10.1016/j.euromechsol.2016.10.003
0997-7538/

the very consideration of this violation is worthwhile. Indeed, the strong ellipticity condition comes from the analysis of the propagation of a plane wave superimposed on the given state of deformation. Intact material can propagate such wave while the damaged material cannot. Thus, the direction of the superimposed wave can tell the story of the direction of failure localization and, ultimately, the crack orientation in the damaged material.

This work addresses two practically interesting calculations concerning the onset of material instability via the loss of ellipticity. First, we consider simple shear of natural rubber. This kind of deformation *approximately* appears in rubber bearings used to isolate structures, like buildings and bridges, from their foundations in order to minimize the destructive effect of earthquake motions. Second, we consider equibiaxial tension of a sheet of aneurysm material. Aneurysms are local dilations in arteries, resembling inflated balloons, that are prone to rupture with high mortality risks. Aneurysms are in the state of biaxial tension and the character of their fracture can help to understand their structure.

2. Theoretical background

In this section, we summarize the theoretical background for the convenience of the reader. More detailed developments can be found in Truesdell and Noll (2004), Antman (1995), and Ogden (1997), for example. Our notation follows Volokh (2016), particularly.

2.1. Initial-boundary-value problem (IBVP)

The initial-boundary-value problem (IBVP) of finite elasticity for incompressible material can be written as follows

$$\begin{aligned}
\rho_0\frac{\partial^2\mathbf{y}}{\partial t^2} &= \mathrm{Div}\mathbf{P}+\mathbf{b}_0,\\
\mathbf{P}\mathbf{F}^{\mathrm{T}} &= \mathbf{F}\mathbf{P}^{\mathrm{T}},\\
\mathbf{P} &= \frac{\partial\psi}{\partial\mathbf{F}}-\mathit{\Pi}\mathbf{F}^{-\mathrm{T}},\\
\det\mathbf{F} &= 1\\
\mathbf{P}\mathbf{n}_0 &= \bar{\mathbf{t}}_0 \quad \text{or} \quad \mathbf{y}=\bar{\mathbf{y}},\\
\mathbf{y}(t=0) &= \mathbf{y}_0,\\
\frac{\partial\mathbf{y}}{\partial t}(t=0) &= \mathbf{v}_0,
\end{aligned} \tag{1}$$

where ρ_0 is the referential mass density; $\mathbf{y}$ is the placement of a material point in the current configuration Ω of a body, which was placed at $\mathbf{x}$ in the reference configuration Ω_0; $\mathbf{P}$ is the first Piola-Kirchhoff stress and $(\mathrm{Div}\mathbf{P})_i=\partial P_{ij}/\partial x_j$; $\mathbf{b}_0$ is the body force per unit reference volume; $\mathbf{F}=\mathrm{Grad}\mathbf{y}(\mathbf{x})$ is the deformation gradient; ψ is the strain energy density per unit reference volume; $\mathit{\Pi}$ is the Lagrange multiplier; $\mathbf{n}_0$ is an outward unit normal to the body surface $\partial\Omega_0$ in the reference configuration; $\bar{\mathbf{t}}_0$ is the prescribed Lagrangean traction on $\partial\Omega_0$; $\bar{\mathbf{y}}$ is the prescribed surface placement; and $\mathbf{y}_0$ and $\mathbf{v}_0$ are the prescribed initial placement and velocity.

Eq. $(1)_{1-2}$ are the linear and angular momenta balance in Ω_0; Eq. $(1)_3$ is the hyperelastic constitutive law; Eq. $(1)_4$ is the incompressibility condition; Eq. $(1)_5$ is the natural or essential boundary condition on $\partial\Omega_0$; Eq. $(1)_{6-7}$ are the initial conditions in Ω_0.

2.2. Incremental IBVP

Let us superimpose small (infinitesimal) increments on placements $\mathbf{y}\to\mathbf{y}+\tilde{\mathbf{y}}$ where tilde designates increment. Then, the incremental Eq. (1) takes form

$$\begin{aligned}
\rho_0\frac{\partial^2\tilde{\mathbf{y}}}{\partial t^2} &= \mathrm{Div}\tilde{\mathbf{P}},\\
\tilde{\mathbf{P}}\mathbf{F}^{\mathrm{T}}+\mathbf{P}\tilde{\mathbf{F}}^{\mathrm{T}} &= \left(\tilde{\mathbf{P}}\mathbf{F}^{\mathrm{T}}+\mathbf{P}\tilde{\mathbf{F}}^{\mathrm{T}}\right)^{\mathrm{T}},\\
\tilde{\mathbf{P}} &= \frac{\partial^2\psi}{\partial\mathbf{F}\partial\mathbf{F}}:\tilde{\mathbf{F}}+\mathit{\Pi}\mathbf{F}^{-\mathrm{T}}\tilde{\mathbf{F}}^{\mathrm{T}}\mathbf{F}^{-\mathrm{T}}-\tilde{\mathit{\Pi}}\mathbf{F}^{-\mathrm{T}},\\
\tilde{\mathbf{F}}:\mathbf{F}^{-\mathrm{T}} &= 0,\\
\tilde{\mathbf{P}}\mathbf{n}_0 &= \mathbf{0} \quad \text{or} \quad \tilde{\mathbf{y}}=\mathbf{0},\\
\tilde{\mathbf{y}}(t=0) &= \mathbf{0},\\
\frac{\partial\tilde{\mathbf{y}}}{\partial t}(t=0) &= \mathbf{0},
\end{aligned} \tag{2}$$

where $\tilde{\mathbf{F}}=\partial\tilde{\mathbf{y}}/\partial\mathbf{x}$; double contraction reads $\mathbf{A}{:}\mathbf{B}=A_{ij}B_{ij}$; and we assume that body force $\mathbf{b}_0$, traction $\bar{\mathbf{t}}_0$, and prescribed placements $\bar{\mathbf{y}}$ are "dead", i.e. they do not depend on deformation.

It is convenient to reformulate the incremental IBVP in the form where the current configuration Ω is the referential one

$$\begin{aligned}
\rho\frac{\partial^2\tilde{\mathbf{y}}}{\partial t^2} &= \mathrm{div}\tilde{\boldsymbol{\sigma}},\\
\tilde{\boldsymbol{\sigma}}+\boldsymbol{\sigma}\tilde{\mathbf{L}}^{\mathrm{T}} &= \left(\tilde{\boldsymbol{\sigma}}+\boldsymbol{\sigma}\tilde{\mathbf{L}}^{\mathrm{T}}\right)^{\mathrm{T}},\\
\tilde{\boldsymbol{\sigma}} &= \mathbb{A}:\tilde{\mathbf{L}}+\mathit{\Pi}\tilde{\mathbf{L}}^{\mathrm{T}}-\tilde{\mathit{\Pi}}\mathbf{1},\\
\tilde{\mathbf{L}}:\mathbf{1} &= 0,\\
\tilde{\boldsymbol{\sigma}}\mathbf{n} &= \mathbf{0} \quad \text{or} \quad \tilde{\mathbf{y}}=\mathbf{0},\\
\tilde{\mathbf{y}}(t=0) &= \mathbf{0},\\
\frac{\partial\tilde{\mathbf{y}}}{\partial t}(t=0) &= \mathbf{0},
\end{aligned} \tag{3}$$

where $(\mathrm{div}\tilde{\boldsymbol{\sigma}})_i=\partial\tilde{\sigma}_{ij}/\partial y_j$; $\mathbf{1}$ is the second-order identity tensor and

$$\begin{aligned}
\rho &= \rho_0,\\
\tilde{\boldsymbol{\sigma}} &= \tilde{\mathbf{P}}\mathbf{F}^{\mathrm{T}},\\
\boldsymbol{\sigma} &= \mathbf{P}\mathbf{F}^{\mathrm{T}},\\
\tilde{\mathbf{L}} &= \tilde{\mathbf{F}}\mathbf{F}^{-1},\\
\mathbf{n} &= \mathbf{F}^{-\mathrm{T}}\mathbf{n}_0\left|\mathbf{F}^{-\mathrm{T}}\mathbf{n}_0\right|^{-1}.
\end{aligned} \tag{4}$$

Eq. $(3)_{1-2}$ are the linear and angular momenta balance in Ω; Eq. $(3)_3$ is the hyperelastic constitutive law; Eq. $(3)_4$ is the incompressibility condition; Eq. $(3)_5$ is the natural or essential boundary condition on $\partial\Omega$; Eq. $(3)_{6-7}$ are the initial conditions in Ω.

In $(3)_3$ we introduced the fourth-order elasticity tensor $\mathbb{A}$ with Cartesian components

$$A_{ijkl}=F_{js}F_{lm}\frac{\partial^2\psi}{\partial F_{is}\partial F_{km}}. \tag{5}$$

In the particular case of the strain energy $\psi(I_1)$ depending only on the first invariant $I_1=\mathbf{F}{:}\mathbf{F}$ we have

$$A_{ijkl}=4\psi_{11}F_{is}F_{km}F_{js}F_{lm}+2\psi_1\delta_{ki}F_{jm}F_{lm}, \tag{6}$$

where

$$\psi_1\equiv\frac{\partial\psi}{\partial I_1},\quad \psi_{11}\equiv\frac{\partial\psi_1}{\partial I_1}.$$

2.3. Superimposed plane wave

In the case of the propagation of plane waves we assume incremental solutions in the form

$$\begin{aligned} \tilde{\mathbf{y}}(\mathbf{y}) &= \mathbf{r}g(\mathbf{s}\cdot\mathbf{y} - wt), \\ \tilde{\Pi} &= \Upsilon g'(\mathbf{s}\cdot\mathbf{y} - wt), \end{aligned} \tag{7}$$

where unit vector $\mathbf{r}$ is called the wave polarization; unit vector $\mathbf{s}$ is the direction of the wave propagation; w is the wave speed; and prime designates differentiation with respect to the argument of function g.

Substituting (7) in the linear momentum balance $(3)_1$ and incompressibility condition $(3)_4$ we obtain respectively

$$\begin{aligned} \rho w^2\mathbf{r} &= \mathbf{\Lambda}(\mathbf{s})\mathbf{r} - \Upsilon\mathbf{s}, \\ \mathbf{r}\cdot\mathbf{s} &= 0, \end{aligned} \tag{8}$$

where

$$\Lambda_{mi} = A_{mnij}s_n s_j \tag{9}$$

is the acoustic tensor.

It should not be missed that the entries of the elasticity tensor $\mathbb{A}$ are uniform for the assumed homogeneous deformation state.

Moreover, we can calculate Υ by taking the scalar product of $(8)_1$ with $\mathbf{s}$

$$\Upsilon = \mathbf{s}\cdot\mathbf{\Lambda}(\mathbf{s})\mathbf{r}. \tag{10}$$

Now, we can rewrite (8) in the form

$$\begin{aligned} \rho w^2\mathbf{r} &= \mathbf{\Lambda}^*(\mathbf{s})\mathbf{r}, \\ \mathbf{r}\cdot\mathbf{s} &= 0, \end{aligned} \tag{11}$$

where

$$\mathbf{\Lambda}^*(\mathbf{s}) = \mathbf{\Lambda}(\mathbf{s}) - \mathbf{s}\otimes\mathbf{\Lambda}(\mathbf{s})\mathbf{s} \tag{12}$$

is the modified acoustic tensor for incompressible material.

We note that $\mathbf{\Lambda}^*(\mathbf{s})$ is not symmetric. It is singular because zero eigenvalue corresponds to the left eigenvector $\mathbf{s}$

$$\mathbf{\Lambda}^{*\mathrm{T}}\mathbf{s} = (\mathbf{\Lambda} - \mathbf{s}\otimes\mathbf{\Lambda}\mathbf{s})^{\mathrm{T}}\mathbf{s} = \mathbf{\Lambda}^{\mathrm{T}}\mathbf{s} - \mathbf{\Lambda}\mathbf{s} = \Big(\mathbf{\Lambda}^{\mathrm{T}} - \mathbf{\Lambda}\Big)\mathbf{s} = 0. \tag{13}$$

Thus, at most, there are two real plane waves and both them are transverse because of the incompressibility condition $(11)_2$.

The scalar product of $(8)_1$ with $\mathbf{r}$ provides the real wave speeds for the strong ellipticity condition

$$\rho w^2 = \mathbf{r}\cdot\mathbf{\Lambda}(\mathbf{s})\mathbf{r} - \Upsilon\mathbf{r}\cdot\mathbf{s} = \mathbf{r}\cdot\mathbf{\Lambda}(\mathbf{s})\mathbf{r} > 0. \tag{14}$$

In the case of the strain energy depending on the first invariant only $\psi(I_1)$ we substitute (6) in the acoustic tensor and we get

$$\Lambda_{ik} = A_{ijkl}s_j s_l = 4\psi_{11}F_{is}F_{km}F_{js}F_{lm}s_j s_l + 2\psi_1\delta_{ki}F_{jm}F_{lm}s_j s_l, \tag{15}$$

or

$$\mathbf{\Lambda}(\mathbf{s}) = 4\psi_{11}(\mathbf{B}\mathbf{s})\otimes(\mathbf{B}\mathbf{s}) + 2\psi_1(\mathbf{s}\cdot\mathbf{B}\mathbf{s})\mathbf{1}, \tag{16}$$

where $\mathbf{B}=\mathbf{F}\mathbf{F}^{\mathrm{T}}$ is the left Cauchy-Green tensor.

The speed of a plane wave can now be calculated as follows

$$\rho w^2 = 4\psi_{11}(\mathbf{r}\cdot\mathbf{B}\mathbf{s})^2 + 2\psi_1(\mathbf{s}\cdot\mathbf{B}\mathbf{s}). \tag{17}$$

2.4. Elasticity with energy limiters

In order to enforce a material failure description, we use the following form of the strain energy function

$$\psi(\mathbf{F},\zeta) = \psi_{\mathrm{f}} - H(\zeta)\psi_{\mathrm{e}}(\mathbf{F}), \tag{18}$$

where

$$\psi_{\mathrm{e}}(\mathbf{F}) = \frac{\Phi}{m}\Gamma\left(\frac{1}{m}, \frac{W(\mathbf{F})^m}{\Phi^m}\right), \quad \psi_{\mathrm{f}} = \psi_{\mathrm{e}}(\mathbf{1}). \tag{19}$$

Here ψ_{f} and $\psi_{\mathrm{e}}(\mathbf{F})$ designate the constant bulk failure energy and the elastic energy respectively; $H(\zeta)$ is a unit step function, i.e. $H(\zeta)=0$ if $\zeta<0$ and $H(\zeta)=1$ otherwise; $\Gamma(s,x) = \int_x^\infty t^{s-1}e^{-t}dt$ is the upper incomplete gamma function; $W(\mathbf{F})$ is the strain energy of intact (without failure) material; Φ is the energy limiter, which is calibrated in macroscopic experiments; and m is a dimensionless material parameter, which controls the sharpness of the transition to material failure on the stress-strain curve. Increasing or decreasing m it is possible to simulate more or less steep ruptures of the internal bonds accordingly.

The switch parameter $\zeta\in(-\infty,0]$ is defined by the evolution equation

$$\dot{\zeta} = -H\left(\varepsilon - \frac{\psi_{\mathrm{e}}}{\psi_{\mathrm{f}}}\right), \quad \zeta(t=0) = 0, \tag{20}$$

where $0<\varepsilon\ll 1$ is a dimensionless precision constant.

The physical interpretation of (18) is straightforward: material response is hyperelastic as long as the strain energy is below its limit - ψ_{f}. When the limit is reached, then the strain energy remains constant for the rest of the deformation process, thereby making material the healing impossible. Parameter ζ is *not an internal variable*. It functions as a switch: if $\zeta=0$ then the process is elastic and if $\zeta<0$ then the material is irreversibly damaged and the strain energy is dissipated.

Constitutive equations can be derived from (18) via a thermodynamic argument. Let us consider the dissipation inequality

$$\mathbf{P} : \dot{\mathbf{F}} - \dot{\psi}(\mathbf{F},\zeta) \geq 0, \tag{21}$$

where $\mathbf{P}$ is the first Piola-Kirchhoff stress tensor.

The energy increment is calculated as follows

$$\dot{\psi}(\mathbf{F},\zeta) = -\delta(\zeta)\dot{\zeta}\psi_{\mathrm{e}}(\mathbf{F}) - H(\zeta)\frac{\partial\psi_{\mathrm{e}}(\mathbf{F})}{\partial\mathbf{F}} : \dot{\mathbf{F}}, \tag{22}$$

where $\delta(\zeta)$ is the Dirac delta.

We notice that

$$\delta(\zeta)\dot{\zeta} = 0 \tag{23}$$

for all values of ζ. Indeed, the case of $\zeta\neq 0$ follows immediately from the definition of Dirac's delta. In the case of $\zeta=0$, we note that the relation $\zeta = \int\dot{\zeta}dt = 0$ along with the definition of $\dot{\zeta}$ as a step function in (20) imply $\dot{\zeta}\equiv 0$ since a non-positive integrand must be identically zero for the integral to vanish.

Substitution of (22) and (23) in the dissipation inequality (21) yields

$$\left(\mathbf{P} + H(\zeta)\frac{\partial\psi_{\mathrm{e}}(\mathbf{F})}{\partial\mathbf{F}}\right) : \dot{\mathbf{F}} \geq 0, \tag{24}$$

and the constitutive equations are obtained following the Coleman-Noll procedure

$$\mathbf{P} = -H(\zeta)\frac{\partial \psi_e(\mathbf{F})}{\partial \mathbf{F}}. \tag{25}$$

The switch parameter ζ does not contribute to the energy increment contrary to the traditional internal variables of damage mechanics. Moreover, it does nor require a threshold condition or physically motivated evolution equation. The introduction of the switch parameter is a purely formal mathematical tool to provide the irreversibility of failure when the failure energy is reached.

We should finally note that the use of the switch parameter is important in the cases of material unloading. The latter cases are not considered in the present work and we can set henceforth

$$\zeta \equiv 0 \Rightarrow H(\zeta) \equiv 1. \tag{26}$$

3. Simple shear in rubber bearings

In simple shear we have

$$y_1 = x_1 + \gamma x_2, \quad y_2 = x_2, \quad y_3 = x_3, \tag{27}$$

and

$$\begin{aligned} \mathbf{F} &= \mathbf{1} + \gamma \mathbf{e}_1 \otimes \mathbf{e}_2, \\ \mathbf{B} &= \mathbf{1} + \gamma(\mathbf{e}_1 \otimes \mathbf{e}_2 + \mathbf{e}_2 \otimes \mathbf{e}_1) + \gamma^2 \mathbf{e}_1 \otimes \mathbf{e}_1. \end{aligned} \tag{28}$$

where $\mathbf{e}_1$,$\mathbf{e}_2$,$\mathbf{e}_3$ are Cartesian basis vectors and γ is amount of shear.

Then, we calculate

$$\begin{aligned} \mathbf{Bs} &= \mathbf{s} + \left(\gamma s_2 + \gamma^2 s_1\right)\mathbf{e}_1 + \gamma s_1 \mathbf{e}_2, \\ \mathbf{s}\cdot\mathbf{Bs} &= 1 + 2\gamma s_2 s_1 + \gamma^2 s_1^2, \\ \mathbf{r}\cdot\mathbf{Bs} &= \gamma s_2 r_1 + \gamma^2 s_1 r_1 + \gamma s_1 r_2, \end{aligned} \tag{29}$$

and, thus, we obtain for the weighted squared wave speed

$$\rho w^2 = 4\psi_{11}\left(\gamma s_2 r_1 + \gamma^2 s_1 r_1 + \gamma s_1 r_2\right)^2 + 2\psi_1\left(1 + 2\gamma s_2 s_1 + \gamma^2 s_1^2\right). \tag{30}$$

Let us further specify the wave direction and polarization vectors accordingly

$$\begin{aligned} \mathbf{s} &= \cos\alpha \mathbf{e}_1 + \sin\alpha \mathbf{e}_2, \\ \mathbf{r} &= -\beta \sin\alpha \mathbf{e}_1 + \beta \cos\alpha \mathbf{e}_2 + \sqrt{1-\beta^2}\mathbf{e}_3, \end{aligned} \tag{31}$$

where α is the angle in plane x_1–x_2 and $0 \le \beta \le 1$ is an arbitrary multiplier.

The wave speed depends on α, β and γ:

$$\rho w^2 = 4\psi_{11}\gamma^2\beta^2\left(\cos^2\alpha - \sin^2\alpha - \gamma\cos\alpha\sin\alpha\right)^2 + 2\psi_1\left(1 + 2\gamma\cos\alpha\sin\alpha + \gamma^2\cos^2\alpha\right). \tag{32}$$

Then, we calculate from (18) ($H \equiv 1$)

$$\begin{aligned} \psi_1 &= W_1 \exp\left(-\frac{W^m}{\Phi^m}\right), \\ \psi_{11} &= \left(W_{11} - \frac{mW^{m-1}}{\Phi^m}W_1^2\right)\exp\left(-\frac{W^m}{\Phi^m}\right), \end{aligned} \tag{33}$$

where we use the Yeoh model for the intact material behavior

$$\begin{aligned} W &= c_1(I_1-3) + c_2(I_1-3)^2 + c_3(I_1-3)^3, \\ W_1 &= c_1 + 2c_2(I_1-3) + 3c_3(I_1-3)^2, \\ W_{11} &= 2c_2 + 6c_3(I_1-3), \end{aligned} \tag{34}$$

and

$$I_1 = 3 + \gamma^2. \tag{35}$$

This model is calibrated as follows (Volokh, 2013) for Natural Rubber vulcanizate

$$\begin{aligned} c_1 &= 0.298 \text{ MPa}, \\ c_2 &= 0.014 \text{ MPa}, \\ c_3 &= 0.00016 \text{ MPa}, \\ \Phi &= 82.0 \text{ MPa}, \\ m &= 10. \end{aligned} \tag{36}$$

The Cauchy stress - stretch curve for the Yeoh model enhanced with the energy limiter is shown in Fig. 1, where also the results are shown for the intact material model. Failure occurs at the limit point at critical stretch λ_{cr}=7.12 in accordance with experimental data from Hamdi et al. (2006).

By using the Yeoh model with the energy limiter it is possible to find the critical failure stretches - the failure envelope - by using the critical condition in the form: $(\partial^2\psi/\partial\lambda_1^2)(\partial^2\psi/\partial\lambda_2^2) - (\partial^2\psi/\partial\lambda_1\partial\lambda_2)^2 = 0$, where λ_1 and λ_2 are axial stretches. Comparison of the theory with the experimental data from Hamdi et al. (2006) is shown in Fig. 2.

Somewhat lower critical stretches in equal biaxial tension are reasonable in view of the high imperfection sensitivity of the experiments.

With account of the material specifications we can find the unknown wave parameters from the condition of the vanishing wave speed

$$\rho w^2 = f_1 f_2 = 0, \tag{37}$$

where

$$\begin{aligned} f_1 &= 4\left(W_{11} - \frac{mW^{m-1}}{\Phi^m}W_1^2\right)\gamma^2\beta^2\left(\cos^2\alpha - \sin^2\alpha - \gamma\cos\alpha\sin\alpha\right)^2 \\ &\quad + 2W_1\left(1 + 2\gamma\cos\alpha\sin\alpha + \gamma^2\cos^2\alpha\right), \\ f_2 &= \exp\left(-\frac{W^m}{\Phi^m}\right). \end{aligned} \tag{38}$$

The split conditions read

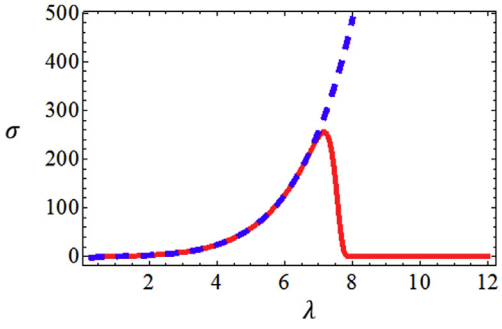

Fig. 1. Cauchy stress [MPa] versus stretch in uniaxial tension of natural rubber: dashed line designates the intact model; solid line designates the model with the energy limiter.

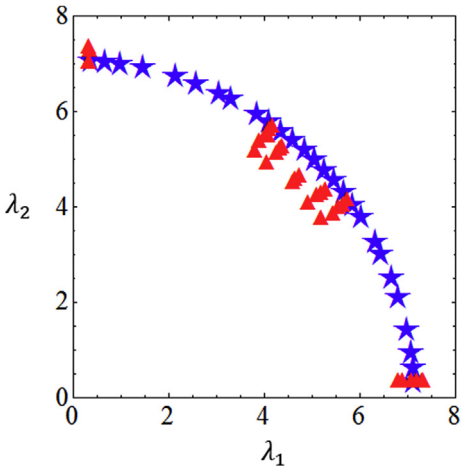

Fig. 2. Failure envelope for biaxial tension of natural rubber: theory (★) versus experiment (▲).

$$f_1 = 0, \quad f_2 = 0. \tag{39}$$

The exponential function f_2 is shown graphically in Fig. 3.

We note that the function converges to zero numerically very fast and the theoretical "infinity" becomes the actual digital one at the starred point.

Thus, the split critical conditions can be represented graphically as two curves in terms of α, β and γ - Fig. 4.

We note that f_2 does not depend on α and β while in the case of f_1 the magnitude of γ increases with the decreasing β. The lowest magnitude of γ=6.92843 is obtained for $\alpha=\pi/2$ or $\alpha=3\pi/2$, which means that failure localizes along axis x_1 or *the crack is expected in the horizontal direction*.

It is interesting to compare the obtained qualitative result with the prediction based on the popular criterion of maximum stress or stretch. The left Cauchy-Green tensor has the following components for γ=6.92843

$$[\mathbf{B}] = \begin{bmatrix} 1+6.92843^2 & 6.92843 & 0 \\ 6.92843 & 1 & 0 \\ 0 & 0 & 1 \end{bmatrix}.$$

Solving the eigenproblem for this matrix we find that the largest principal stretch occurs in direction

$$0.99\mathbf{e}_1 + 0.14\mathbf{e}_2,$$

which almost coincides with x_1. The latter means that the *crack is expected in the vertical direction*, that is along axis x_2.

Remarkably, we have quite opposite predictions based on the strong ellipticity and maximum stretch criteria. Unfortunately, we do not have the experimental data for the considered material. The

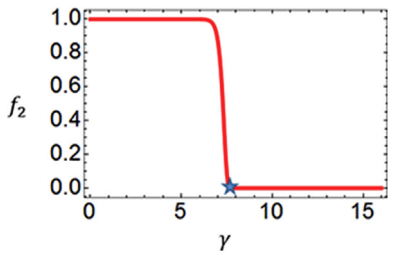

Fig. 3. Convergence of the exponential function $f_2(\gamma)$ to zero.

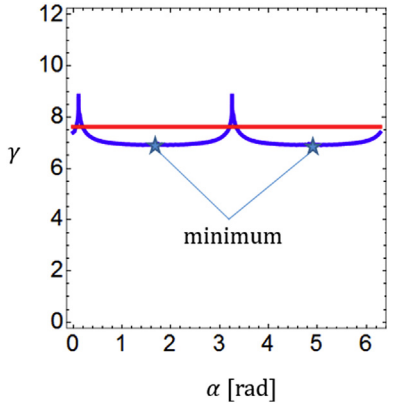

Fig. 4. Dependence of the amount of shear on the orientation of the superimposed acoustic wave. Curves f_1=0 (β=1) and f_2=0 are presented in blue and red accordingly. The minimum amount of shear shown by stars corresponds to the onset of instability via the loss of ellipticity. (For interpretation of the references to colour in this figure legend, the reader is referred to the web version of this article.)

"best approximation" of simple shear failure available in the literature is shown in Fig. 5.

Although the appearance of the horizontal crack is in a good agreement with the previous analysis the comparison is mainly *qualitative*. The reason is that the material of the real rubber bearing is different from natural rubber. Besides, we ignored the pressure from the bridge assuming that deformations triggered by the pressure were much smaller than the deformations triggered by the earth movement. Of course, a more realistic numerical study would be interesting. The latter study would go far beyond the scope of the present note.

4. Equibiaxial tension in aneurysms

In the case of equibiaxial tension of aneurysm material we have

$$y_1 = \lambda x_1, \quad y_2 = \lambda x_2, \quad y_3 = \lambda^{-2} x_3, \tag{40}$$

where λ is the stretch in the direction of tension.

The deformation gradient and the left Cauchy-Green tensor take the following forms accordingly

$$\begin{aligned} \mathbf{F} &= \lambda \mathbf{e}_1 \otimes \mathbf{e}_1 + \lambda \mathbf{e}_2 \otimes \mathbf{e}_2 + \lambda^{-2} \mathbf{e}_3 \otimes \mathbf{e}_3, \\ \mathbf{B} &= \lambda^2 \mathbf{e}_1 \otimes \mathbf{e}_1 + \lambda^2 \mathbf{e}_2 \otimes \mathbf{e}_2 + \lambda^{-4} \mathbf{e}_3 \otimes \mathbf{e}_3. \end{aligned} \tag{41}$$

Then, we calculate

$$\begin{aligned} \mathbf{Bs} &= \lambda^2 \mathbf{e}_1 s_1 + \lambda^2 \mathbf{e}_2 s_2 + \lambda^{-4} \mathbf{e}_3 s_3, \\ \mathbf{s}\cdot\mathbf{Bs} &= \lambda^2 s_1^2 + \lambda^2 s_2^2 + \lambda^{-4} s_3^2, \\ \mathbf{r}\cdot\mathbf{Bs} &= \lambda^2 r_1 s_1 + \lambda^2 r_2 s_2 + \lambda^{-4} r_3 s_3, \end{aligned} \tag{42}$$

and, thus, we have for the weighted squared wave speed

$$\rho w^2 = 4\psi_{11}\left(\lambda^2 r_1 s_1 + \lambda^2 r_2 s_2 + \lambda^{-4} r_3 s_3\right)^2 + 2\psi_1\left(\lambda^2 s_1^2 + \lambda^2 s_2^2 + \lambda^{-4} s_3^2\right), \tag{43}$$

Substitution of the wave direction and polarization vectors from (31) yields

$$\rho w^2 = 2\psi_1 \lambda^2. \tag{44}$$

Similar to the case of the rubber bearing we use the reduced

Fig. 5. Fracture of the bridge rubber bearing after the 2011 Great East Japan Earthquake (From Takahashi, 2012). Horizontal cracks are observed on the right.

intact Yeoh strain energy enhanced with the energy limiter and calibrate the model as follows (Volokh, 2015)

$$W = c_1(I_1 - 3) + c_2(I_1 - 3)^2, \tag{45}$$

where

$$c_1 = 0.52 \text{ MPa}, \; c_2 = 3.82 \text{ MPa}, \; \Phi = 0.255 \text{ MPa}, \; m = 1. \tag{46}$$

It is possible to reduce the Yeoh model in the case of the aneurysm because of much smaller stretches. A reasonable experimental fit in the latter case can be done with less constants.

The Cauchy stress - stretch curve for this constitutive model is shown in Fig. 6, where also the experimental data from Raghavan and Vorp (2000) is presented.

With account of the latter specification we can find the critical parameters α, β and λ of the loss of ellipticity from the condition of zero wave speed

$$\rho w^2 = f_1 f_2 = 0, \tag{47}$$

where

$$f_1 = 2\left\{c_1 + 2c_2\left(2\lambda^2 + \lambda^{-4} - 3\right)\right\}\lambda^2,$$
$$f_2 = \exp\left[-\left(c_1\left(2\lambda^2 + \lambda^{-4} - 3\right) + c_2\left(2\lambda^2 + \lambda^{-4} - 3\right)^2\right)^m \Phi^{-m}\right]. \tag{48}$$

We note that $f_1>0$ for $\lambda>1$ and, consequently, the ellipticity is lost for $f_2=0$ - Fig. 7.

We note that in the latter case the critical stretch and the loss of ellipticity do not depend on the wave direction and polarization. The latter means that the failure localization or crack can happen in any direction and there is an infinite bifurcation multiplicity. It is clear intuitively that " something" needs to break symmetry. We gave a formal basis for the latter notion. No such calculations, to the best of our knowledge, have been done in the literature previously.

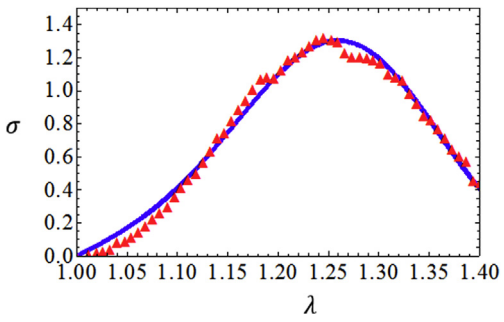

Fig. 6. Cauchy stress [MPa] versus stretch for theory and experiment (▲) in uniaxial tension of AAA material.

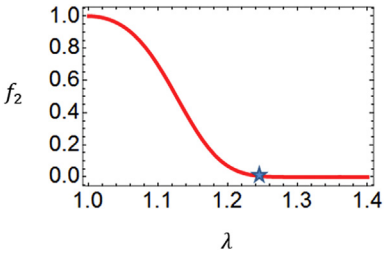

Fig. 7. Convergence of the exponential function $f_2(\gamma)$ to zero.

5. Discussion

We used elasticity with energy limiters to analyze the onset of material instability via the loss of ellipticity in soft solids. Two practically interesting cases were considered. The first was the natural rubber in the state of simple shear. The latter state *approximately* corresponds to the loading of rubber bearings used in buildings and bridges to isolate the main structure from the ground motion during the earthquakes. We found that failure localized in horizontal direction, parallel to the shearing, in perfect qualitative correspondence with the field observations after earthquakes. Second, we considered equibiaxial tension of an aneurysm. We found that the isotropic aneurysm material exhibited infinitely many possible directions of failure localization in equibiaxial tension. The latter means that the random direction of cracks in equibiaxial tension experiment, e.g. membrane inflation, can be an indicator of material isotropy. Consequently, a preferable direction of the crack alignment can be interpreted as an indicator of the aneurysm anisotropy.

Acknowledgement

The support from the Israel Science Foundation (ISF-198/15) is gratefully acknowledged.

References

Antman, S.S., 1995. Nonlinear Problems of Elasticity. Springer.
Dal, H., Kaliske, M., 2009. A micro-continuum-mechanical material model for failure of rubber- like materials: application to ageing-induced fracturing. J. Mech. Phys. Solids 57, 1340–1356.
Danescu, A., 1991. Bifurcation in the traction problem for a transversely isotropic material. Math. Proc. Camb. Philos. Soc. 110, 385–394.
de Souza Neto, E.A., Peric, D., Owen, D.R.J., 1998. Continuum modeling and numerical simulation of material damage at finite strains. Arch. Comp. Meth Eng. 5, 311–384.
De Tommasi, D., Puglisi, G., Saccomandi, G., 2008. Localized versus diffuse damage in amorphous materials. Phys. Rev. Lett. 100, 085502.

Dorfmann, A., Ogden, R.W., 2004. A constitutive model for the Mullins effect with permanent set in particle-reinforced rubber. Int. J. Solids Struct. 41, 1855–1878.
Dorfmann, L., Ogden, R.W. (Eds.), 2015. Nonlinear Mechanics of Soft Fibrous Materials. Springer.
Govindjee, S., Simo, J.C., 1991. A micro-mechanically based continuum damage model of carbon black-filled rubbers incorporating the Mullins effect. J. Mech. Phys. Solids 39, 87–112.
Guo, Z., Sluys, L., 2006. Computational modeling of the stress-softening phenomenon of rubber-like materials under cyclic loading. Eur. J. Mech. A/Solids 25, 877–896.
Hamdi, A., Nait Abdelaziz, M., Ait Hocine, N., Heuillet, P., Benseddiq, N., 2006. A fracture criterion of rubber-like materials under plane stress conditions. Polym. Test. 25, 994–1005.
Johnson, M.A., Beatty, M.F., 1993. A constitutive equation for the Mullins effect in stress controlled uniaxial extension experiments. Cont. Mech. Therm. 5, 301–318.
Kaliske, M., Nasdala, L., Rothert, H., 2001. On damage modeling for elastic and viscoelastic materials at large strain. Comp. Struct. 79, 2133–2141.
Kurashige, M., 1981. Instability of a transversely isotropic elastic slab subjected to axial loads. J. Appl. Mech. 48, 351–356.
Menzel, A., Steinmann, P., 2001. A theoretical and computational framework for anisotropic continuum damage mechanics at large strains. Int. J. Solids Struct. 38, 9505–9523.
Merodio, J., Ogden, R.W., 2002. Material instabilities in fiber-reinforced nonlinearly elastic solids under plane deformation. Arch. Mech. 54, 525–552.
Merodio, J., Ogden, R.W., 2003. Instabilities and loss of ellipticity in fiber-reinforced compressible non-linearly elastic solids under plane deformation. Int. J. Solids Struct. 40, 4707–4727.
Merodio, J., Ogden, R.W., 2005. Mechanical response of fiber-reinforced incompressible non-linearly elastic solids. Int. J. Non-Linear Mech. 40, 213–227.
Miehe, C., 1995. Discontinuous and continuous damage evolution in Ogden-type large-strain elastic materials. Eur. J. Mech. A/Solids 14, 697–720.
Ogden, R.W., 1997. Non-Linear Elastic Deformations. Dover.
Ogden, R.W., Roxburgh, D.G., 1999. A pseudo–elastic model for the Mullins effect in filled rubber. Proc. Roy. Soc. Lond. Ser. A 455, 2861–2877.
Raghavan, M.L., Vorp, D.A., 2000. Toward a biomechanical tool to evaluate rupture potential of abdominal aortic aneurysm: identification of a finite strain constitutive model and evaluation of its applicability. J. Biomech. 33, 475–482.
Simo, J.C., 1987. On a fully three-dimensional finite strain viscoelastic damage model: formulation and computational aspects. Comp. Meth Appl. Mech. Eng. 60, 153–173.
Simo, J.C., Ju, J., 1987. Strain-and stress-based continuum damage models—I. Formul. Int. J. Solids Struct. 23, 821–840.
Takahashi, Y., 2012. Damage of rubber bearings and dumpers of bridges in 2011 great East Japan earthquake. In: Proceedings of the International Symposium on Engineering Lessons Learned from the 2011 Great East Japan Earthquake, March 1-4, 2012, Tokyo, Japan.
Triantafyllidis, N., Abeyaratne, R., 1983. Instability of a finitely deformed fiber-reinforced elastic material. J. Appl. Mech. 50, 149–156.
Truesdell, C., Noll, W., 2004. The Non-Linear Field Theories of Mechanics. Springer.
Volokh, K.Y., 2004. Nonlinear elasticity for modeling fracture of isotropic brittle solids. J. Appl. Mech. 71, 141–143.
Volokh, K.Y., 2007. Hyperelasticity with softening for modeling materials failure. J. Mech. Phys. Solids 55, 2237–2264.
Volokh, K.Y., 2013. Review of the energy limiters approach to modeling failure of rubber. Rubber Chem. Technol. 86, 470–487.
Volokh, K.Y., 2014. On irreversibility and dissipation in hyperelasticity with softening. J. Appl. Mech. 81, 074501.
Volokh, K.Y., 2015. Cavitation instability as a trigger of aneurysm rupture. Biomech. Model Mechanobiol. 14, 1071–1079.
Volokh, K.Y., 2016. Mechanics of Soft Materials. Springer.